BIOMOLECULES & THERAPEUTICS

Original Article
Biomol Ther 26(6), 599-607 (2018)

Fasiglifam (TAK-875), a G Protein-Coupled Receptor 40 (GPR40) Agonist, May Induce Hepatotoxicity through Reactive Oxygen Species Generation in a GPR40-Dependent Manner

MinJeong Kim[1,†], Gyo Jeong Gu[2,†], Yun-Sook Koh[1], Su-Hyun Lee[3], Yi Rang Na[2], Seung Hyeok Seok[2,*] and Kyung-Min Lim[1,*]

[1]College of Pharmacology, Ewha Womans University, Seoul 03760,
[2]Department of Microbiology and Immunology and Institute of Endemic Disease, Seoul National University College of Medicine, Seoul 03080,
[3]Biosolutions Co., Seoul 01811, Republic of Korea

Abstract

Fasiglifam (TAK-875) a G-protein coupled receptor 40 (GPR40) agonist, significantly improves hyperglycemia without hypoglycemia and weight gain, the major side effects of conventional anti-diabetics. Unfortunately, during multi-center Phase 3 clinical trials, unexpected liver toxicity resulted in premature termination of its development. Here, we investigated whether TAK-875 directly inflicts toxicity on hepatocytes and explored its underlying mechanism of toxicity. TAK-875 decreased viability of 2D and 3D cultures of HepG2, a human hepatocarcinoma cell line, in concentration- (>50 μM) and time-dependent manners, both of which corresponded with ROS generation. An antioxidant, N-acetylcysteine, attenuated TAK-875-mediated hepatotoxicity, which confirmed the role of ROS generation. Of note, knockdown of GPR40 using siRNA abolished the hepatotoxicity of TAK-875 and attenuated ROS generation. In contrast, TAK-875 induced no cytotoxicity in fibroblasts up to 500 μM. Supporting the hepatotoxic potential of TAK-875, exposure to TAK-875 resulted in increased mortality of zebrafish larvae at 25 μM. Histopathological examination of zebrafish exposed to TAK-875 revealed severe hepatotoxicity as manifested by degenerated hypertrophic hepatocytes with cytoplasmic vacuolation and acentric nuclei, confirming that TAK-875 may induce direct hepatotoxicity and that ROS generation may be involved in a GPR40-dependent manner.

Key Words: Fasiglifam, Hepatotoxicity, Zebrafish, Reactive oxygen species, GPR40, G-protein coupled receptor 40

INTRODUCTION

As the average life-span is being extended, the prevalence of diabetes mellitus is escalating (Nanditha *et al*., 2016). With an increasing number of patients (382 million people worldwide in 2013), the drug market for anti-diabetics has grown enormously, establishing a multi-billion dollar market in US alone (Stephens *et al*., 2006). To address this, new anti-diabetics with novel therapeutic mechanisms are being actively explored (Gallwitz, 2016). Among these, agonists of GPR40 (also known as free fatty acid receptor 1 [FFAR1]), a G-protein coupled receptor (GPCR) for long-chain fatty acids, received the spotlight since they, unlike other conventional anti-diabetics including sulfonylurea or glinide, selectively stimulate insulin secretion only in hyperglycemic conditions (Bramlage *et al*., 2012). GPR40 agonists activate GPR40 expressed on β-cells, leading to the secretion of incretins, GLP-1 (glucagon like peptide1) and GIP (glucose-dependent insulin tropic polypeptide), and insulin in a glucose-dependent manner (Christiansen *et al*., 2008). This distinct and ideal therapeutic profile of GPR40 agonists avoids hypoglycemia and body weight increase, which are common and serious side effects of conventional anti-diabetics (Tsujihata *et al*., 2011).

Among the tens of drug candidates targeting GPR40 currently on track for nonclinical/clinical development (Kamiyama and Terauchi, 2015), fasiglifam, TAK-875, was a leading can-

Open Access **https://doi.org/10.4062/biomolther.2017.225**

This is an Open Access article distributed under the terms of the Creative Commons Attribution Non-Commercial License (http://creativecommons.org/licenses/by-nc/4.0/) which permits unrestricted non-commercial use, distribution, and reproduction in any medium, provided the original work is properly cited.

Received Nov 1, 2017 **Revised** Jan 11, 2018 **Accepted** Jan 12, 2018
Published Online Feb 12, 2018

***Corresponding Authors**
E-mail: kmlim@ewha.ac.kr (Lim KM), lamseok@snu.ac.kr (Seok SH)
Tel: +82-2-3277-3055 (Lim KM), +82-2-740-8302 (Seok SH)
Fax: +82-2-3277-3760 (Lim KM), +82-2-743-0881 (Seok SH)
[†]The first two authors contributed equally to this work.

Copyright © 2018 The Korean Society of Applied Pharmacology

didate. Its activity was demonstrated in both disease models (Ito *et al*., 2016) and clinical trials (Kaku *et al*., 2015) wherein significant improvement was observed against hyperglycemia without the serious side effects of hypoglycemia and weight gain, making TAK-875 superior to conventional anti-diabetics such as glinides or sulfonylureas (Naik *et al*., 2012). More importantly, blood HbA1C levels, a crucial marker for chronic diabetes, were significantly improved in patients who took either 25 or 50 mg TAK-875 without major adverse effects (Naik *et al*., 2012). However, in a global multi-center phase 3 study, unexpected liver toxicity was reported, which resulted in the premature termination of TAK-875 development (Watterson *et al*., 2014).

It is widely known that diabetes is accompanied by various complications including retinopathy (UK Prospective Diabetes Study Group, 1998), nephropathy (Adler *et al*., 2003), and hepatic diseases (Morling *et al*., 2016). The risk of hepatic diseases such as liver fibrosis, liver cancer, and chronic liver dysfunction, is significantly higher in Type 2 diabetics as compared to healthy people, which has been well demonstrated in large-scaled epidemiological studies (Chen *et al*., 2015; Kwok *et al*., 2015). Similarly, high levels of oxidative stress (Saeidnia and Abdollahi, 2013) and compromised liver function or dysfunction of diabetic patients resulted in increased susceptibility to liver toxicity of anti-diabetic drugs (Chitturi and George, 2001; El-serag *et al*., 2004; Gupte *et al*., 2004). Exemplifying this, some anti-diabetic drugs such as troglitazone, metformin and TAK-875 showed concern for drug-induced hepatotoxicity, which has resulted in warning, termination of clinical trials and withdrawal from the market (Gitlin *et al*., 1998; Halegoua-De Marzio and Navarro, 2013; Shah *et al*., 2015).

The mechanism of TAK-875-induced hepatotoxicity and whether it is GPR40-dependent or from off-target effects has yet to be established (Mancini and Poitout, 2015). GPR40 is expressed in many organs and tissues as well as in the pancreas (Steneberg *et al*., 2005; Schnell *et al*., 2007). GPR40 expression has been reported in a variety of tissues, including intestinal enteroendocrine cells I, K, and L and even the brain (Christiansen *et al*., 2010). The expression of GPR40 in the liver has been demonstrated, where it was shown to promote the effects of insulin (Ou *et al*., 2013). Accordingly, a possible role of GPR40 in TAK-875-induced hepatotoxicity cannot be excluded. Recently, it was shown that TAK-875 and TAK-875 acyl glucuronide affect bile transporters like Ntcp and OATP/Oatp (uptake transporters) and MRP2/Mrp2 (efflux transporter), leading to cholestatic liver toxicity and hyperbilirubinemia (Li *et al*., 2015; Otieno *et al*., 2018). However, it remains to be elucidated whether TAK-875 inflicts direct toxicity on hepatocytes.

In the present study, we employed 2D and 3D HepG2 culture models *in vitro* to evaluate the direct hepatotoxicity of TAK-875. To further elucidate the mechanisms underlying TAK-875 induced cytotoxicity in HepG2 cells, the generation of reactive oxygen species (ROS) and effects of GPR40 knockdown were investigated as well as comparison of the cytotoxicity of TAK-875 in a non-liver fibroblast cell line. Lastly we confirmed the induction of hepatotoxicity of TAK-875 using zebrafish larvae to investigate the relevance of our findings in a system close to *in vivo*.

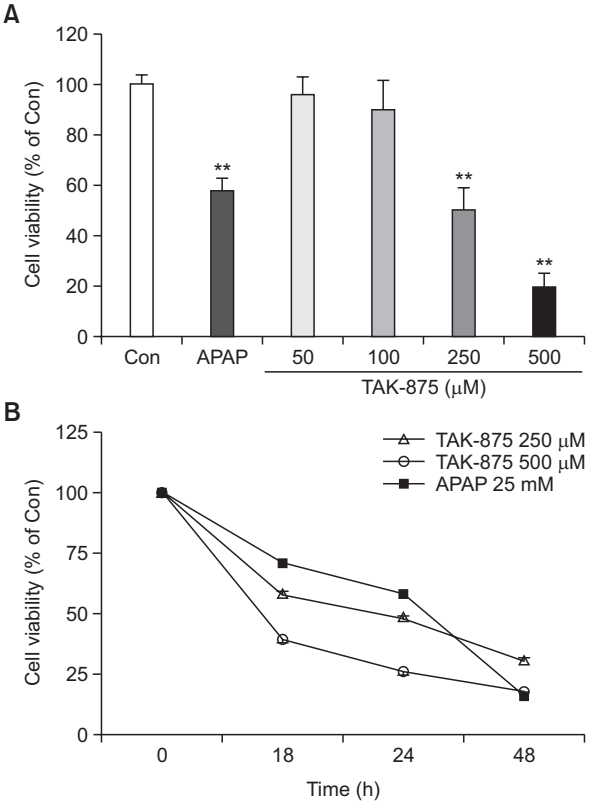

Fig. 1. TAK-875-induced cytotoxicity against HepG2 cells (2D monolayer). (A) Dose-dependent (at 24 h) and (B) Time-dependent toxicity of TAK875 compared to APAP 25 mM as measured by WST-1 assay. Data shown are mean ± SE of at least 3 replications. $^{**}p<0.01$.

MATERIALS AND METHODS

Chemicals

Fasiglifam, TAK-875 , with >99% purity was kindly provided by the SK Chemical (Sungnam, Korea), and acetaminophen (APAP) was from Sigma-Aldrich (St. Louis, MO, USA). Chemicals were dissolved in DMSO to prepare stock solutions for experiments, and final DMSO concentrations did not exceed 0.5%.

Cell culture and cell treatment

HepG2 cell line: The human hepatocarcinoma (HepG2) cell line was purchased form ATCC (American Type Culture Collection, Rockville, MD, USA). The cells were cultivated in Dulbecco's modified essential medium (DMEM, Sigma-Aldrich) supplemented with 10% fetal bovine serum (FBS) and antibiotics (100 U/mL of penicillin A and 100 U/mL of streptomycin) at 37°C in a humidified atmosphere with 5% CO_2. The medium was replenished every 2 days. After confluence, the cells were sub-cultured following trypsinization.

HepG2 3D spheres were prepared according to a previously described method (Kim *et al*., 2018). Briefly, HepG2 cells were seeded into a 96 well ultra-low attachment plate at a density of 1×10^8 cells/well and were cultivated for 14 days. The medium was changed three times each week.

Human dermal fibroblasts (HDFs): Primary HDFs were

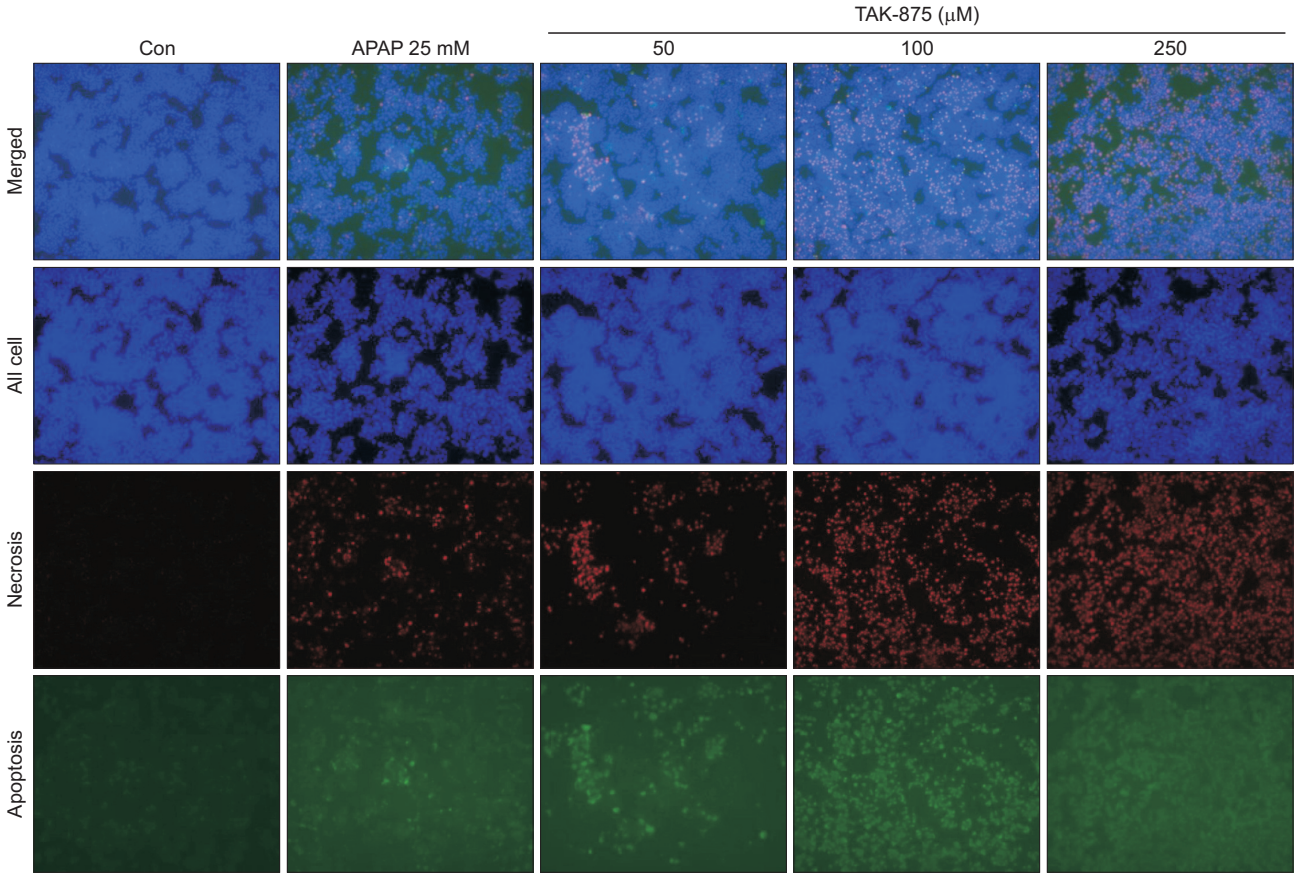

Fig. 2. TAK-875 induced apoptosis and necrosis in HepG2 cells. The visualization of healthy (blue), necrotic (red), or apoptotic (green) cells following treatment with DMSO, TAK875, or APAP 25 mM (at 24 h), respectively, in HepG2 cells using a triple fluorescence staining kit under fluorescence microscope (100×).

obtained from Biosolution Co., Ltd. (Seoul, Korea). Cells were cultured as described previously (Song *et al*., 2017) in DMEM supplemented with antibiotics (100 U/ml of penicillin A and 100 U/ml of streptomycin) and 10% FBS at 37°C in a humidified atmosphere containing 5% CO_2; 60% confluent cells were cultured in serum-free medium for 24 h.

Cell treatment: Cells were treated with various concentrations of TAK-875, APAP, or DMSO (final 0.5%) in culture medium for 24 h. The control group was treated with 0.5% DMSO only. Fibroblasts were seeded into 6 well plates at a density of 1.5×10^5/well, while HepG2 cells were seeded at 1.0×10^4/well in 96 well plates. For ROS determination, each cell line was seeded at 1.5×10^5/well in 6 well plates.

MTT and WST-1 assay for cell viability

Cell viability was determined using either the 3-[4, 5-dimethylthiazol-2-yl]-2. 5-diphenyl-tetrazolium bromide (MTT; Sigma-Aldrich) or the WST-1 (4-[3-(4-iodophenyl)-2-(4-nitrophenyl)-2H-5-tetrazolio]-1,3-benzenedisulfonate) (Roche, Indianapolis, IN, USA) assay, which are based on the reduction of tetrazolium into formazan dye by active mitochondria (Lee *et al*., 2017). After treatment, the medium was removed, and the cells were incubated with 250 μl of MTT (0.3 mg/mL in serum-free medium) or 100 μl of WST-1 (final 10 μg/ml in PBS) for 3 h at 37°C and were protected from light. For MTT, formazan products were dissolved in 300 μl DMSO with gentle shaking for 30 min at 37°C. For MTT, 200 μl of supernatants were transferred into 96-well plates, and absorbance was determined by microplate spectrophotometry at 540 nm (Molecular Devices Inc., Sunnyvale, CA, USA). For WST-1, absorbance was measured at 450 nm. Cell viability was calculated using the following formula:

Cell viability (%)
=mean value of treated group/control group×100 (%).

Detection of healthy, apoptotic, and necrotic cells

Cells undergoing apoptosis and necrosis were visualized using a commercial fluorescence triple staining kit comprised of Hoechst 33258, annexin, and ethidium bromide (Promo Kine Apoptotic/Necrotic Cells Detection Kit, Promo Cell GmBH, Heidelberg, Germany) under a fluorescence microscope (Axiovert 200 M microscope, Carl Zeiss, Oberkochen, Germany) as described previously (Hwang *et al*., 2018). Briefly, cells were washed with 1x binding buffer and stained by adding 5 μL of FITC-Annexin V and 5 μL of EthD-III to 100 μL 1X binding buffer. Samples were incubated with the staining solution for 15 min at room temperature and were protected from light.

Measurement of reactive oxygen species production

Production of ROS was measured using a 2′,7′-dichloroflu-

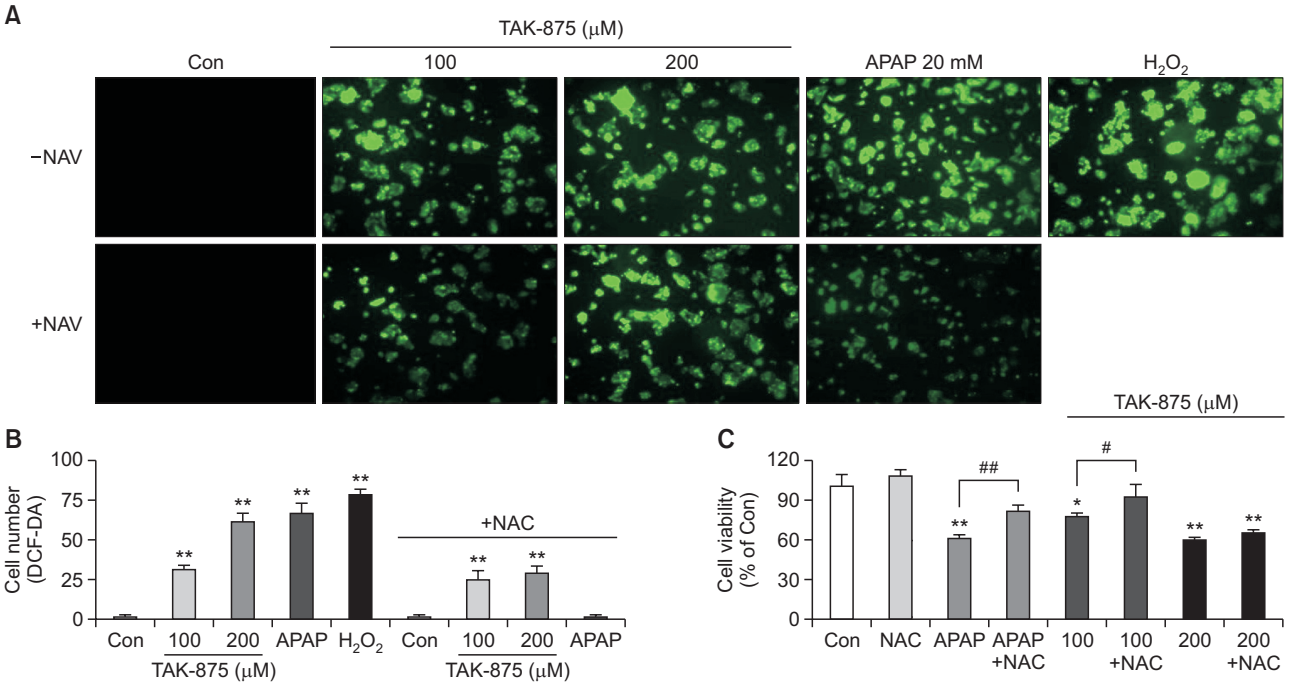

Fig. 3. TAK875-induced ROS generation in HepG2 cells (2D monolayer) *in vitro*. Cells were exposed to TAK875 (100, 200 μM) or APAP 20 mM with or without NAC 5 mM for 24 h or were treated with H_2O_2 100 μM for 10 min as a positive control for ROS generation. (A) ROS generation was detected using a fluorescence microscopy (×200) with DCF-DA enhanced fluorescence. (B) DCF-DA enhanced fluorescence-positive cells were analyzed with image-J software. (C) Cell viability was measured using the WST-1 assay. Data are mean ± SE of at least 3 replications. **p*<0.05, ***p*<0.01, versus DMSO control. $^{\#}p$<0.05, versus TAK875 100 μM, $^{\#\#}p$<0.01, versus APAP.

orescein-diacetate (DCF-DA, Eugene, OR, USA)-enhanced fluorescence assay as described previously (Kim *et al*., 2016). Briefly, HepG2 cells were pretreated with the indicated concentrations of TAK-875 and APAP with or without N-acetyl cysteine (NAC) 5 mM for 24 h, washed with PBS, and stained with 5 μM DCF-DA for 10 min at 37°C. For the positive control, cells were treated with 100 μM H_2O_2 for 10 min before staining. The resulting cells were visualized using the Softmax5.2 program under an Axiovert 200M microscope (Zeiss, Oberkochen, Germany). Cellular fluorescence was measured using the Image J program (NIH, Bethesda, MD, USA).

Knockdown of GPR40 through siRNA application in HepG2

To knock out GPR40, HepG2 cells were seeded onto 35mm dishes at a density of 2.5x10^5 cells/well and cultured for 24 h in a 37°C 5% CO_2 incubator. The siRNA mixture [5 μM; GPR40: ON-TARGETplus FFAR1 siRNA (human)], L-005571-02-0005, positive control: ON-TARGETplus GAPDH control pool – human, D-001830-10-05, negative control: ON-TARGETplus Non-targeting pool, D-001810-10-05) with DharmaFECT agent (GE Dharmacon, Lafayette, CO, USA) in serum free media were added to the cells, and the cells were further incubated for 48 h. Knockdown of GPR40 was confirmed through PCR analysis after extraction with Trizol reagent (Invitrogen, CARLSBAD, CA, USA). The concentration of RNA was determined using a NanoDrop 1000 spectrophotometer (NanoDrop Technologies, Inc., Wilmington, DE, USA).

Reverse transcription-PCR

Relative expression levels of mRNAs were measured by PCR. Total RNA, extracted from HepG2 cell treated with siRNA, was used to synthesize cDNA using the pre-master mix with oligo dT (Bioepis, Seoul, Korea). Semi-quantitative RT-PCR was performed using electrophoresis though a 1.5% agarose gel with eco dye (EcoDye DNA staining solution, Biofact, Daejeon, Korea). The sequence of primers of HepG2 was as follows: forward GPR40, 5′-GTGTCACCTGGGTCTGGTCT-3′; reverse GPR40, 5′-GAGCAGGAGAGAGAGGCTGA-3′; forward Human GAPDH, 5′-GGTCACCAGGGCTGCTTTTA-3′; reverse Human GAPDH, 5′-TTCCCGTTCTCAGCCTTGAC-3′; cycling parameters were 95°C for 2 min, and then 33 cycles of 95°C for 20 s, 54°C for 40 s, and 72°C for 30 s, followed by 72°C for 5 min.

Hepatotoxicity testing with zebrafish embryo

Maintenance of zebrafish: Zebrafish (*Danio rerio*) were maintained under a 14 h light/10 h dark cycle in an automatic circulating tank system and fed brine shrimp three times per day (Nirwane *et al*., 2016; Jeong *et al*., 2018). Three or four pairs of zebrafish were set up for mating, and approximately 200-300 embryos were generated. Embryos were maintained at 28°C in egg water. Experiments were performed on hatched zebrafish embryos at 3 days post fertilization (dpf). All animal studies were performed in accordance with the international rules considering animal experiments and the internationally accepted ethical principles for laboratory animal use and care. The protocols were approved by the Institutional Animal Care and Use Committee of the Seoul National University (accession number SNU-151029-4).

Chemical treatment: Five zebrafish embryos per well at 3 dpf were immersed in 500 μL of egg water containing 0.1 mM 1-phenyl-2-thiourea (PTU) solution for 48-72 h on a 24-well

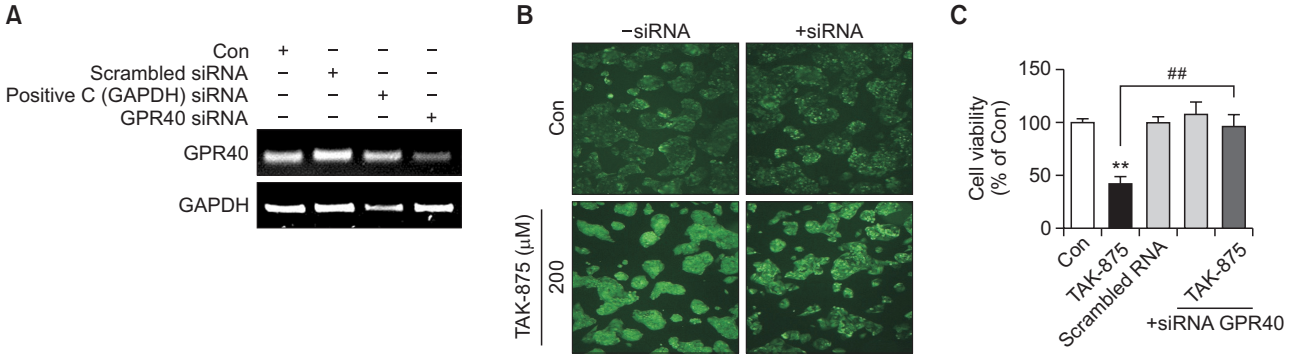

Fig. 4. Effects of GPR40 knockdown on TAK875-induced ROS generation and hepatoxicity in HepG2 cells. GPR40 was knocked-down using siRNA treatment for 48 h. (A) Knock-down was confirmed by PCR. (B) ROS generation (200x) and (C) cytotoxicity were examined in GPR40 Knock-down HepG2 cells as described above. Viability was measured by the WST-1 assay. Data are mean ± SE of at least 3 replications. $^{**}p<0.01$, versus DMSO control, $^{\#\#}p<0.01$, versus TAK875.

plate. TAK-875, acetaminophen, or 0.1% DMSO for vehicle control was added into PTU solution depending on each experimental design. Survival rates were observed every 6 h, and dead embryos were removed.

Morphological assessment of hepatotoxicity in zebrafish: To assess hepatotoxicity morphologically, zebrafish larvae were mounted in 1% low melting agarose. Images were obtained using a stereomicroscope (Leica M165 FC) to obtain liver and yolk sac sizes. Liver size and yolk sac retention were calculated using the formulas:

Liver size (% of control)
=liver area (chemical)/liver area (control)×100%

Yolk sac retention (% of control)
=yolk sac area (chemical)/yolk sac area (control)×100%

Liver histology in zebrafish: Zebrafish larvae were collected and fixed in 10% neutral buffered formalin at room temperature overnight and were then subjected to paraffin embedding and sectioning. Hematoxylin and eosin staining was performed to histologically examine hepatotoxicity as described previously (Jeong *et al*., 2017a; Kim *et al*., 2017).

Statistics

Results are presented as mean ± SE of three or more independent experiments. Statistical significance of differences between groups was assessed using a two-tailed Student's t-test using GraphPad Prism 5 (GraphPad Software, San Diego, CA, USA). A p-value<0.05 was considered statistically significant.

RESULTS

To evaluate the cytotoxicity of fasiglifam, TAK-875, against hepatocytes, a human hepatocarcinoma cell line, HepG2, cultured in a monolayer was treated with various concentrations of TAK-875 and acetaminophen 20 mM (APAP) as a positive control for 24 h, and, thereafter, cell viability was measured. TAK-875 decreased cell viability of HepG2 cells in both concentration- and time-dependent manners from a concentration of ~100 μM, suggesting that it might cause direct hepatotoxicity (Fig. 1). This level of cytotoxicity against HepG2 was similar to that induced by APAP at ~20 mM, reflecting that the potency of hepatotoxicity of TAK-875 may be much stronger than that of APAP. Visualization of apoptotic and necrotic cells revealed that TAK-875 exposed-HepG2 cells exhibited late apoptotic (green & red) appearance as was found with APAP (Fig. 2).

We assessed the generation of reactive oxygen species (ROS) employing DCF-DA enhanced fluorescence to examine the mechanism underlying the hepatotoxicity of TAK-875. We measured cell viability and detected changes in intracellular ROS generation following the treatment of HepG2 with TAK-875. Intracellular ROS production increased significantly in HepG2 exposed to TAK-875 as compared with those exposed to H_2O_2 and APAP, two positive controls well known for their toxic mechanisms associated with ROS production (Fig. 3A, 3B). HepG2 treated with TAK-875 plus N-acetylcysteine (NAC), an antioxidant, resulted in significant reduction of ROS production (Fig. 3B) and alleviation of the cytotoxicity of TAK-875 (Fig. 3C).

TAK-875 is a GPR40 agonist. To identify the role of GPR40 in the manifestation of cytotoxicity of TAK-875, GPR40 was knock-downed using siRNA (Fig. 4A). TAK-875-induced ROS generation was significantly attenuated after knockdown of GPR40 (Fig. 4B). This was further confirmed by the abrogation of TAK-875-induced cytotoxicity in HepG2 cells (Fig. 4C). To examine whether the cytotoxicity of TAK-875 was common to other cell-types, human dermal fibroblasts considered not to express GPR40 (Fujita *et al*., 2011; Bahar Halpern *et al*., 2012), were treated with TAK-875 and cell viability and ROS production were evaluated. TAK-875 did not induce cytotoxicity or ROS generation in fibroblasts, which was in clear contrast to the findings in HepG2 cells (Fig. 5A, 5B).

A 3D HepG2 culture, a spheroid system, has recently been used to study the hepatotoxicity of xenobiotics. We cultivated HepG2 in spheroid, and the hepatotoxicity of TAK-875 was assessed. APAP, a positive control, induced significant levels of cytotoxicity from the concentrations of 25 mM while TAK-875 manifested from 250-500 μM (Fig. 6A). This was further corroborated by histological examination of treated spheroids wherein chromatin condensation and unclear demarcation were evident in APAP or TAK-875 treated spheroids (Fig. 6B). However, neither potentiation nor inhibition of cytotoxicity was observed, suggesting that the contribution of metabolism may

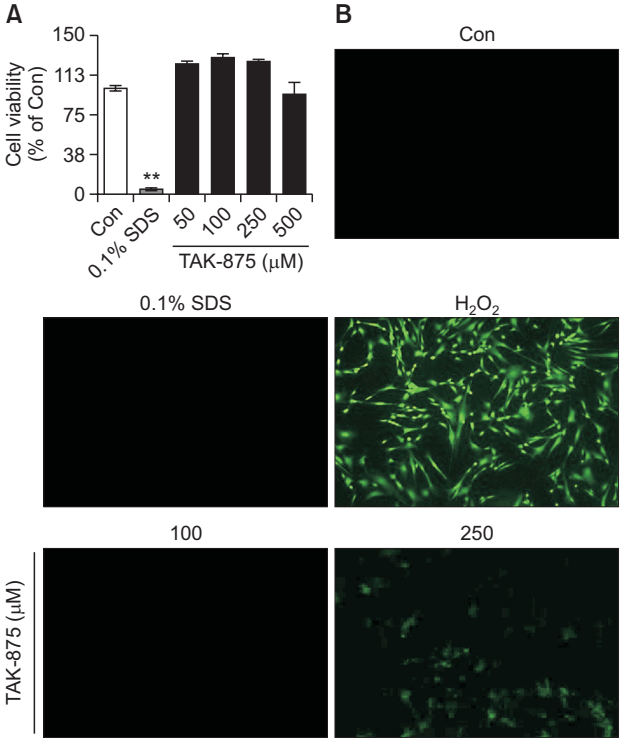

Fig. 5. Effects of TAK-875 on cell viability and ROS generation in a human dermal fibroblast (2D monolayer). Cells were exposed to TAK-875 (50, 100, 250 or 500 μM) or 0.1% SDS for 24 h and (A) cell viability was measured by MTT assay. (B) ROS generation was evaluated using DCF-DA enhanced fluorescence (100x magnification). H_2O_2 100 μM for 10 min as a positive control for ROS generation. Data are mean ± SE of at least 3 replications. ***p*<0.01.

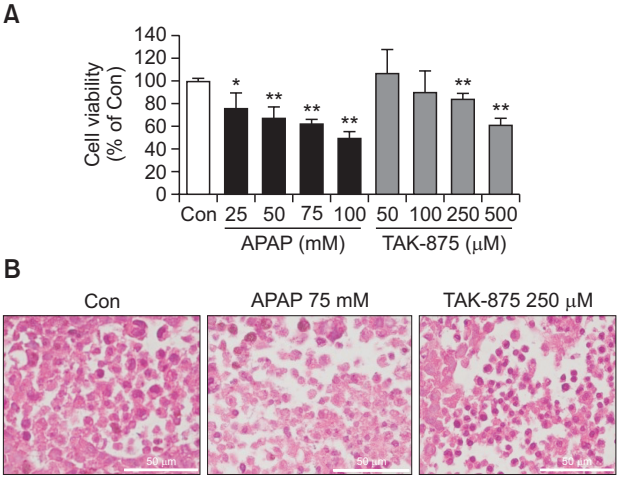

Fig. 6. TAK-875-induced cytotoxicity against HepG2 spheroids. HepG2 spheroids were prepared over 2 weeks of cultivation and exposed to APAP or TAK-875 for 24 h. (A) Cell viability was measured using the WST-1 assay (n=3, Data is mean ± SE), and (B) histology was examined (H&E staining, 400x, bar=50 μm). **p*<0.05, ***p*<0.01, versus DMSO control.

be minimal.

Liver consists of various types of cells, including Kupffer cells, stellate cells, and parenchymal hepatocytes. 2D or 3D single cell culture models have limitations for addressing interactions between various cell types in the liver or interaction between liver and other organs. To explore the potential systemic effects involved in the manifestation of hepatotoxicity of TAK-875, zebrafish, a non-mammalian alternative to animal test widely used for liver physiology (Saad *et al*., 2017) and hepatotoxicity owing to its similarity to human liver (Goldstone *et al*., 2010) was employed as a surrogate *in vivo* model to assess the hepatotoxicity of TAK-875. First, we examined survival rates of TAK-875 exposed zebrafish larvae. APAP served as a positive drug inducing hepatotoxicity in zebrafish larvae (Vliegenthart *et al*., 2014). APAP barely induced mortality up to the 5 mM concentration. However, TAK-875 exposed zebrafish larvae showed significant mortality from 24 h of chemical treatment with increased responses depending on the concentration (Fig. 7A, 7B).

We assessed hepatotoxicity by determining morphological changes in the liver and yolk sac (Fig. 8) after exposure to APAP or TAK-875. Because liver size can be reduced in response to various pathologies such as inflammation, degeneration, and necrosis (He *et al*., 2013a), we assumed that drug induced hepatotoxicity could be quantitated by measuring liver size (Fig. 8A). As expected, both APAP and TAK-875 significantly reduced liver sizes of zebrafish larvae compared to the vehicle control (Fig. 8B). In addition, we observed the delayed yolk absorption with significantly larger yolk retentions in TAK-875 and APAP exposed zebrafish larvae. These results suggest that TAK-875 and APAP impaired liver function of zebrafish larvae resulting in reduced metabolism of lipid absorbed mostly from yolk in the liver (He *et al*., 2013a).

Finally we histologically evaluated TAK-875-induced hepatotoxicity (Fig. 8C). Normal zebrafish larvae livers were filled with well-delineated polygonal hepatocytes with well-preserved cytoplasm and prominent nuclei. However, APAP- and TAK-875-exposed zebrafish larvae showed typical hepatotoxic findings, demonstrating that most of the hepatocytes in these livers had marked vacuolated and enlarged cytoplasm and eccentric nuclei. Collectively, these data confirmed that TAK-875 induces liver damage in a zebrafish model.

DISCUSSION

Here we demonstrated that TAK-875 induced cytotoxicity in HepG2 cells cultured in 2D monolayers or 3D spheroids and that the potency TAK-875 was almost 100 fold stronger than that of APAP. Interestingly, the toxic range of TAK-875 was ~100 μM, which is in a proximate range with the therapeutic level of 10 μM (Cmax, 2.3 μg/mL at 50 mg) suggesting that the margin of safety was small. The cytotoxicity of TAK-875 appeared to be, at least in part, ROS-mediated and GPR40 dependent. Most importantly, the hepatotoxicity of TAK-875 is well-illustrated in zebrafish embryos where treatment with 25 μM TAK-875 resulted in considerable mortality and severe liver damage. The toxic level of TAK-875 is thousands of fold lower than the toxic concentration of APAP in zebrafish and around two fold that of the therapeutic level, demonstrating that the hepatotoxicity of TAK-875 may have biological and clinical relevance.

The mechanism underlying TAK-875-induced hepatotoxicity remains unclear. Li *et al*. (2015) reported that rats receiv-

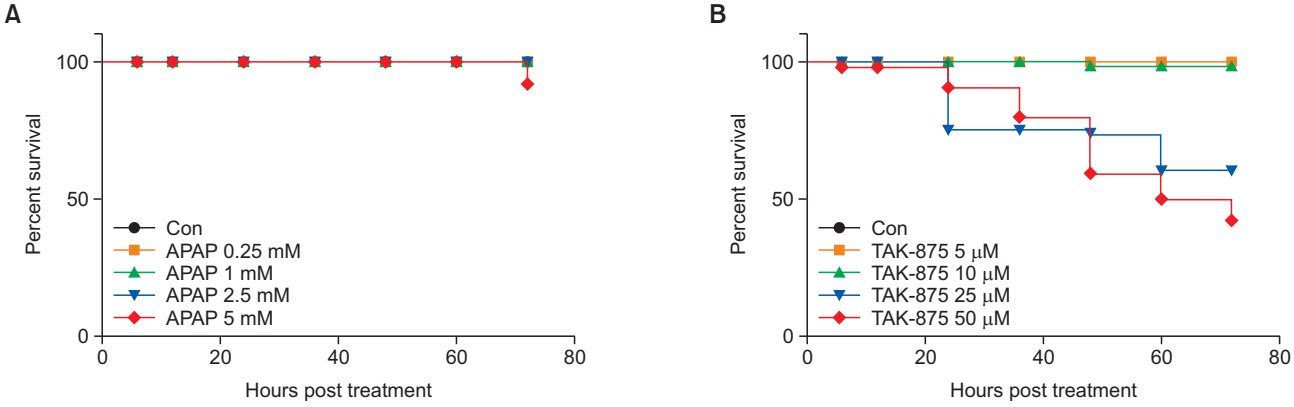

Fig. 7. Survival curves of APAP and TAK-875 exposed zebrafish larvae. Zebrafish larvae at 3 days post fertilization were immersed in egg water containing the indicated concentrations of APAP (A) or TAK-875 (B) and were counted for survival rates for 72 h. Representatives for three independent experiments. n=50 per group.

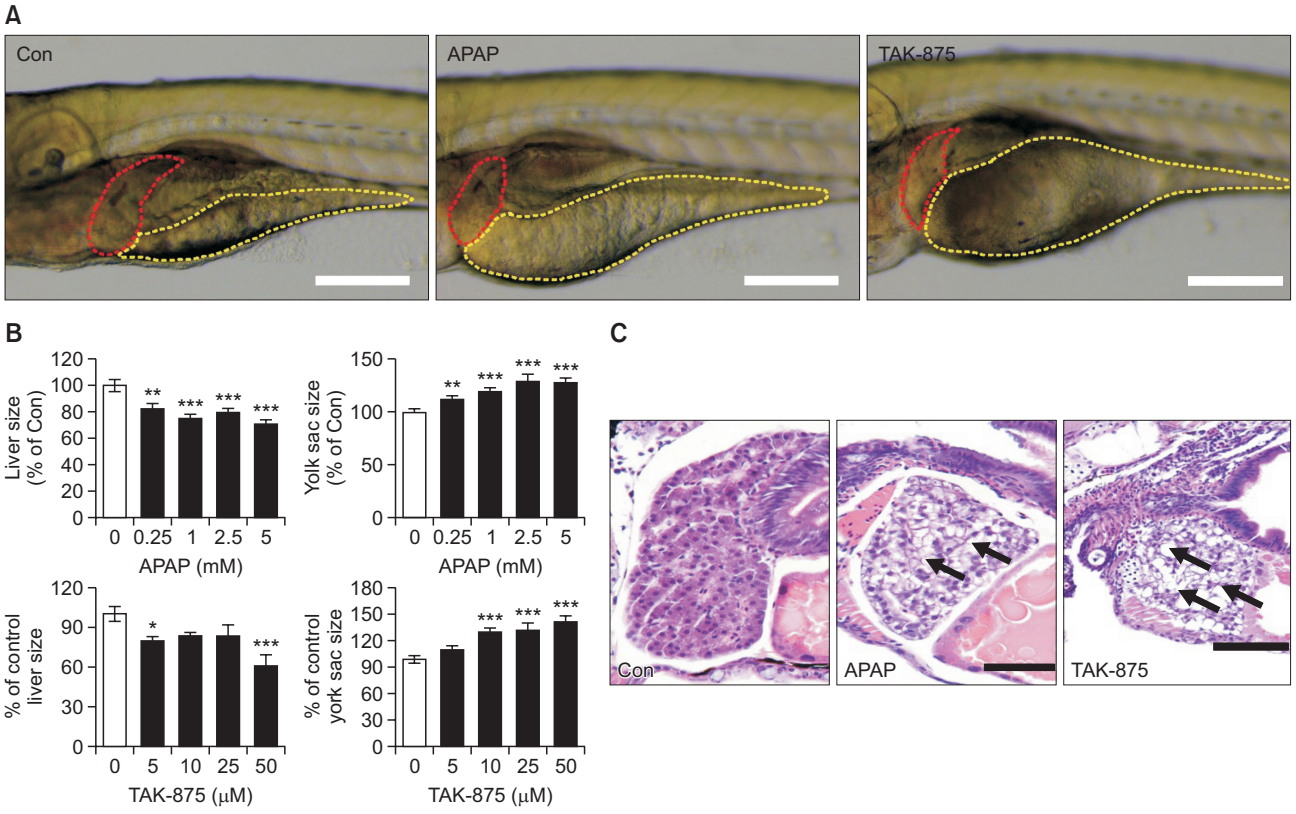

Fig. 8. Morphological assessment of hepatotoxicity on zebrafish larvae exposed to APAP and TAK-875. Zebrafish larvae at 3 days post fertilization were immersed in egg water containing APAP or TAK-875 for 48 h. After drug exposure, the lateral view of zebrafish larvae was imaged for quantitating liver and yolk sizes. (A) Representative images of the lateral view were obtained from vehicle (0.1% DMSO) or drug-exposed zebrafish larvae (APAP 5 mM or TAK-875 10 μM). Red and yellow dotted lines indicate the outer margins of the liver and yolk sac, respectively. Scale bar=200 μm. (B) Relative percentage changes of liver and yolk sizes obtained from APAP and TAK-875 exposed zebrafish larvae were quantitated compared to vehicle control. Data are mean±SE, n=15-20, *p<0.05, **p<0.005, ***p<0.001. (C) H&E stained liver histology was obtained after formal formalin fixation. Black arrows indicate hypertrophic vacuolated hepatocytes with eccentric nuclei. Scale bar=40 μm.

ing TAK-875 exhibited cholestatic hepatotoxicity, which they ascribed to abnormal activities of bile transporters like Ntcp and OATP/Oatp (uptake transporters) and MRP2/Mrp2 (efflux transporter). Very recently, Otieno *et al*. (2018) showed that a reactive acylglucronide metabolite of TAK can be produced with a capacity to induce covalent binding and to inhibit mitochondrial respiration. Here, we demonstrated that ROS generation may be involved in the hepatotoxicity of TAK-875;

this has been further confirmed by the reversal of toxicity of TAK-875 with the antioxidant NAC. Interestingly, in fibroblasts, TAK-875 failed to induce cytotoxicity and ROS generation suggesting that a hepatocyte-selective cytotoxic mechanism may exist, an issue that must be addressed in the future.

TAK-875 directly induced cytotoxicity against HepG2 cells at much lower concentrations than APAP, a representative therapeutic drug with well-established hepatotoxicity concerns. Considering the therapeutic levels of TAK-875 (plasma Cmax 2.3 μg/mL, ~ 5-10 μM), the safety margin is around 25-50 fold. Actually, the effective concentration of APAP is approximately 20-40 μg/mL (corresponding to around 125-250 μM), and the toxic level is around 25 mM, resulting in a toxicity margin of 50 to 100 fold, which gives extra weight to the probable induction of TAK-875 hepatotoxicity in humans. Moreover, considering that a single or intermittent dose regimen of APAP for analgesic or antipyretic purposes is used in relatively healthy people, the repeated intake of TAK-875 to lower blood glucose in the chronically ill diabetic patients who frequently have compromised liver functions may prominently increase the chance of liver injury.

The zebrafish genome has 70% homology with that of humans, and many studies have successfully evaluated and elucidated the hepatotoxicity of xenobiotics using zebrafish (Hill, 2011). Liver toxicity in zebrafish is commonly evaluated through examination of morphological endpoints that include liver degeneration, changes in size, liver shape, and yolk sac retention (He *et al*., 2013b). TAK-875 and APAP caused typical signs of hepatotoxicity in zebrafish livers including reduction in liver size and impaired yolk sac absorption. Interestingly, TAK-875 induced hepatotoxicity at much lower concentrations in zebrafish *in vivo* than in HepG2 cells *in vitro*. This discrepancy could be attributable to the contribution from other cell types in the liver, to the interaction between the liver and other organs, or to species differences.

Since the recent termination of the clinical development of TAK-875, a GPR40 agonist, studies regarding associations between TAK-875 and hepatotoxicity are scarce. Otieno *et al*. (2018) speculated that other GPR40 agonists may not be free from hepatotoxicity but this is largely because of the presence of carboxylic group in their structures, which can produce reactive acylglucuronide as observed in TAK-875. We confirmed that TAK-875 may cause hepatotoxicity through increasing cytosolic ROS generation in hepatocytes, a process that is GPR40-dependent. Resistance of fibroblasts to TAK-875-induced cytotoxicity may support this further. Furthermore, the hepatotoxicity of TAK-875 was demonstrated in zebrafish larvae at the exposure levels relevant to therapeutic doses in humans. These findings may provide important clues to reveal the mechanism of hepatotoxicity of TAK-875 although further studies are necessary to elucidate the pathways for GPR40-dependent ROS generation.

CONFLICT OF INTEREST

There are no conflict of interest.

ACKNOWLEDGMENTS

This work is supported by National Research Foundation of Korea (Grant No. NRF-2015R1D1A1A01057931 and 2017R1A6A3A11034070).

REFERENCES

Adler, A. I., Stevens, R. J., Manley, S. E., Bilous, R. W., Cull, C. A. and Holman, R. R. (2003) Development and progression of nephropathy in type 2 diabetes: the United Kingdom Prospective Diabetes Study (UKPDS 64) *Kidney Int.* **63**, 225-232.

Bahar Halpern, K., Veprik, A., Rubins, N., Naaman, O. and Walker, M. D. (2012) GPR41 gene expression is mediated by internal ribosome entry site (IRES)-dependent translation of bicistronic mRNA encoding GPR40 and GPR41 proteins. *J. Biol. Chem.* **287**, 20154-20163.

Bramlage, P., Gitt, A. K., Binz, C., Krekler, M., Deeg, E. and Tschöpe, D. (2012) Oral antidiabetic treatment in type-2 diabetes in the elderly: balancing the need for glucose control and the risk of hypoglycemia. *Cardiovasc. Diabetol.* **11**, 122.

Chen, J., Han, Y., Xu, C., Xiao, T. and Wang, B. (2015) Effect of type 2 diabetes mellitus on the risk for hepatocellular carcinoma in chronic liver diseases: a meta-analysis of cohort studies. *Eur. J. Cancer Prev.* **24**, 89-99.

Chitturi, S. and George, J. (2001) Hepatotoxicity of commonly used drugs: nonsteroidal anti-inflammatory drugs, antihypertensives, antidiabetic agents, anticonvulsants, lipid-lowering agents, psychotropic drugs. In Seminars in Liver Disease, vol. 22, pp. 169-183.

Christiansen, E., Due-Hansen, M. E., Urban, C., Merten, N., Pfleiderer, M., Karlsen, K. K., Rasmussen, S. S., Steensgaard, M., Hamacher, A. and Schmidt, J. (2010) Structure-activity study of dihydrocinnamic acids and discovery of the potent FFA1 (GPR40) agonist TUG-469. *ACS Med. Chem. Lett.* **1**, 345-349.

Christiansen, E., Urban, C., Merten, N., Liebscher, K., Karlsen, K. K., Hamacher, A., Spinrath, A., Bond, A. D., Drewke, C. and Ullrich, S. (2008) Discovery of potent and selective agonists for the free fatty acid receptor 1 (FFA1/GPR40), a potential target for the treatment of type II diabetes. *J. Med. Chem.* **51**, 7061-7064.

El-serag, H. B., Tran, T. and Everhart, J. E. (2004) Diabetes increases the risk of chronic liver disease and hepatocellular carcinoma. *Gastroenterology* **126**, 460-468.

Fujita, T., Matsuoka, T., Honda, T., Kabashima, K., Hirata, T. and Narumiya, S. (2011) A GPR40 agonist GW9508 suppresses CCL5, CCL17, and CXCL10 induction in keratinocytes and attenuates cutaneous immune inflammation. *J. Invest. Dermatol.* **131**, 1660-1667.

Gallwitz, B. (2016) Novel therapeutic approaches in diabetes. In Novelties in Diabetes, vol. 31, pp. 43-56. Karger Publishers.

Gitlin, N., Julie, N. L., Spurr, C. L., Lim, K. N. and Juarbe, H. M. (1998) Two cases of severe clinical and histologic hepatotoxicity associated with troglitazone. *Ann. Intern. Med.* **129**, 36-38.

Goldstone, J. V., McArthur, A. G., Kubota, A., Zanette, J., Parente, T., Jonsson, M. E., Nelson, D. R. and Stegeman, J. J. (2010) Identification and developmental expression of the full complement of Cytochrome P450 genes in Zebrafish. *BMC Genomics* **11**, 643.

Gupte, P., Amarapurkar, D., Agal, S., Baijal, R., Kulshrestha, P., Pramanik, S., Patel, N., Madan, A. and Amarapurkar, A. (2004) Non-alcoholic steatohepatitis in type 2 diabetes mellitus. *J. Gastroenterol. Hepatol.* **19**, 854-858.

Halegoua-De Marzio, D. and Navarro, V. J. (2013) Hepatotoxicity of cardiovascular and antidiabetic drugs. In Drug-Induced Liver Disease, 3rd ed., pp. 519-540. Elsevier.

He, J. H., Guo, S. Y., Zhu, F., Zhu, J. J., Chen, Y. X., Huang, C. J., Gao, J. M., Dong, Q. X., Xuan, Y. X. and Li, C. Q. (2013b) A zebrafish phenotypic assay for assessing drug-induced hepatotoxicity. *J. Pharmacol. Toxicol. Methods* **67**, 25-32.

He, J.-H., Guo, S.-Y., Zhu, F., Zhu, J.-J., Chen, Y.-X., Huang, C.-J., Gao, J.-M., Dong, Q.-X., Xuan, Y.-X. and Li, C.-Q. (2013a) A zebrafish phenotypic assay for assessing drug-induced hepatotoxicity. *J. Pharmacol. Toxicol. Methods* **67**, 25-32.

Hill, A. (2011) Hepatotoxicity testing in larval zebrafish. In Zebrafish: Methods for Assessing Drug Safety and Toxicity, pp. 89-102. John

Wiley & Sons, Inc., Hoboken, NJ, USA.
Hwang, J. H., Park, H., Choi, D. W., Nam, K. T. and Lim, K. M. (2018) Investigation of dermal toxicity of ionic liquids in monolayer-cultured skin cells and 3D reconstructed human skin models. *Toxicol. In Vitro* **46**, 194-202.
Ito, R., Tsujihata, Y., Suzuki, M., Miyawaki, K., Matsuda, K. and Takeuchi, K. (2016) Fasiglifam/TAK-875, a selective GPR40 agonist, improves hyperglycemia in rats unresponsive to sulfonylureas and acts additively with sulfonylureas. *J. Pharmacol. Exp. Ther.* **357**, 217-227.
Jeong, J. S., Nam, K. T., Lee, B., Pamungkas, A. D., Song, D., Kim, M., Yu, W. J., Lee, J., Jee, S., Park, Y. H. and Lim, K. M. (2017a) Low-dose bisphenol A increases bile duct proliferation in juvenile rats: a possible evidence for risk of liver cancer in the exposed population? *Biomol. Ther. (Seoul)* **25**, 545-552.
Jeong, J. W., Cha, H. J., Han, M. H., Hwang, S. J., Lee, D. S., Yoo, J. S., Choi, I. W., Kim, S., Kim, H. S., Kim, G. Y., Hong, S. H., Park, C., Lee, H. J. and Choi, Y. H. (2018) Spermidine protects against oxidative stress in inflammation models using macrophages and zebrafish. *Biomol. Ther. (Seoul)* **26**, 146-156.
Kaku, K., Enya, K., Nakaya, R., Ohira, T. and Matsuno, R. (2015) Efficacy and safety of fasiglifam (TAK-875), a G protein-coupled receptor 40 agonist, in Japanese patients with type 2 diabetes inadequately controlled by diet and exercise: a randomized, double-blind, placebo-controlled, phase III trial. *Diabetes Obes. Metab.* **17**, 675-681.
Kamiyama, H. and Terauchi, Y. (2015) Current status of clinical development of novel anti-diabetic drugs. *Nihon Rinsho* **73**, 517-522.
Kim, M., Baek, H. S., Lee, M., Park, H., Shin, S. S., Choi, D. W. and Lim, K. M. (2016) Rhododenol and raspberry ketone impair the normal proliferation of melanocytes through reactive oxygen species-dependent activation of GADD45. *Toxicol. In Vitro* **32**, 339-346.
Kim, M., Yun, J. W., Shin, K., Cho, Y., Yang, M., Nam, K. T. and Lim, K. M. (2017) Expression levels of GABA-A receptor subunit alpha 3, gabra3 and lipoprotein lipase, Lpl are associated with the susceptibility to acetaminophen-induced hepatotoxicity. *Biomol. Ther. (Seoul)* **25**, 112-121.
Kim, S., Mun, G. I., Choi, E., Kim, M., Jeong, J. S., Kang, K. W., Jee, S., Lim, K. M. and Lee, Y. S. (2018) Submicromolar bisphenol A induces proliferation and DNA damage in human hepatocyte cell lines in vitro and in juvenile rats in vivo. *Food Chem. Toxicol.* **111**, 125-132.
Kwok, R., Choi, K. C., Wong, G. L., Zhang, Y., Chan, H. L., Luk, A. O., Shu, S. S., Chan, A. W., Yeung, M. W., Chan, J. C., Kong, A. P. and Wong, V. W. (2015) Screening diabetic patients for non-alcoholic fatty liver disease with controlled attenuation parameter and liver stiffness measurements: a prospective cohort study. *Gut* **65**, 1359-1368.
Lee, M., Nam, K. T., Kim, J., Lim, S. E., Yeon, S. H., Lee, B., Lee, J. Y. and Lim, K. M. (2017) Evaluation of ocular irritancy of coal-tar dyes used in cosmetics employing reconstructed human cornea-like epithelium and short time exposure tests. *Food Chem. Toxicol.* **108**, 236-243.
Li, X., Zhong, K., Guo, Z., Zhong, D. and Chen, X. (2015) Fasiglifam (TAK-875) inhibits hepatobiliary transporters: a possible factor contributing to fasiglifam-induced liver injury. *Drug Metab. Dispos.* **43**, 1751-1759.
Mancini, A. and Poitout, V. (2015) GPR40 agonists for the treatment of type 2 diabetes: life after 'TAKing' a hit. *Diabetes Obes. Metab.* **17**, 622-629.
Morling, J. R., Fallowfield, J. A., Guha, I. N., Williamson, R. M., Ali, M., Glancy, S., Strachan, M. W. and Price, J. F. (2016) Clinically significant chronic liver disease in people with Type 2 diabetes: the Edinburgh Type 2 Diabetes Study. *QJM* **109**, 249-256.
Naik, H., Vakilynejad, M., Wu, J., Viswanathan, P., Dote, N., Higuchi, T. and Leifke, E. (2012) Safety, tolerability, pharmacokinetics, and pharmacodynamic properties of the GPR40 agonist TAK-875: results from a double-blind, placebo-controlled single oral dose rising study in healthy volunteers. *J. Clin. Pharmacol.* **52**, 1007-1016.
Nanditha, A., Ma, R. C., Ramachandran, A., Snehalatha, C., Chan, J. C., Chia, K. S., Shaw, J. E. and Zimmet, P. Z. (2016) Diabetes in Asia and the Pacific: implications for the global epidemic. *Diabetes Care* **39**, 472-485.
Nirwane, A., Sridhar, V. and Majumdar, A. (2016) Neurobehavioural changes and brain oxidative stress induced by acute exposure to GSM900 mobile phone radiations in zebrafish (*Danio rerio*) *Toxicol. Res.* **32**, 123-132.
Otieno, M. A., Snoeys, J., Lam, W., Ghosh, A., Player, M. R., Pocai, A., Salter, R., Simic, D., Skaggs, H., Singh, B. and Lim, H. K. (2018) Fasiglifam (TAK-875): mechanistic investigation and retrospective identification of hazards for drug induced liver injury. *Toxicol. Sci.* **163**, 374-384.
Ou, H.-Y., Wu, H.-T., Hung, H.-C., Yang, Y.-C., Wu, J.-S. and Chang, C.-J. (2013) Multiple mechanisms of GW-9508, a selective G protein-coupled receptor 40 agonist, in the regulation of glucose homeostasis and insulin sensitivity. *Am. J. Physiol. Endocrinol. Metab.* **304**, E668-E676.
Saad, M., Matheeussen, A., Bijttebier, S., Verbueken, E., Pype, C., Casteleyn, C., Van Ginneken, C., Apers, S., Maes, L., Cos, P. and Van Cruchten, S. (2017) In vitro CYP-mediated drug metabolism in the zebrafish (embryo) using human reference compounds. *Toxicol. In Vitro* **42**, 329-336.
Saeidnia, S. and Abdollahi, M. (2013) Toxicological and pharmacological concerns on oxidative stress and related diseases. *Toxicol. Appl. Pharmacol.* **273**, 442-455.
Schnell, S., Schaefer, M. and Schöfl, C. (2007) Free fatty acids increase cytosolic free calcium and stimulate insulin secretion from β-cells through activation of GPR40. *Mol. Cell. Endocrinol.* **263**, 173-180.
Shah, F., Leung, L., Barton, H. A., Will, Y., Rodrigues, A. D., Greene, N. and Aleo, M. D. (2015) Setting clinical exposure levels of concern for drug-induced liver injury (DILI) using mechanistic in vitro assays. *Toxicol. Sci.* **147**, 500-514.
Song, D., Park, H., Lee, S. H., Kim, M. J., Kim, E. J. and Lim, K. M. (2017) PAL-12, a new anti-aging hexa-peptoid, inhibits UVB-induced photoaging in human dermal fibroblasts and 3D reconstructed human full skin model, Keraskin-FT. Arch. *Dermatol. Res.* **309**, 697-707.
Steneberg, P., Rubins, N., Bartoov-Shifman, R., Walker, M. D. and Edlund, H. (2005) The FFA receptor GPR40 links hyperinsulinemia, hepatic steatosis, and impaired glucose homeostasis in mouse. *Cell Metab.* **1**, 245-258.
Stephens, J. M., Botteman, M. F. and Hay, J. W. (2006) Economic impact of antidiabetic medications and glycemic control on managed care organizations: a review of the literature. *J. Manag. Care Pharm.* **12**, 130-142.
Tsujihata, Y., Ito, R., Suzuki, M., Harada, A., Negoro, N., Yasuma, T., Momose, Y. and Takeuchi, K. (2011) TAK-875, an orally available G protein-coupled receptor 40/free fatty acid receptor 1 agonist, enhances glucose-dependent insulin secretion and improves both postprandial and fasting hyperglycemia in type 2 diabetic rats. *J. Pharmacol. Exp. Ther.* **339**, 228-237.
UK Prospective Diabetes Study Group (1998) Tight blood pressure control and risk of macrovascular and microvascular complications in type 2 diabetes: UKPDS 38. *BMJ* **317**, 703.
Vliegenthart, A., Tucker, C. S., Del Pozo, J. and Dear, J. W. (2014) Zebrafish as model organisms for studying drug-induced liver injury. *Br. J. Clin. Pharmacol.* **78**, 1217-1227.
Watterson, K. R., Hudson, B. D., Ulven, T. and Milligan, G. (2014) Treatment of type 2 diabetes by free fatty acid receptor agonists. *Front. Endocrinol. (Lausanne)* **5**, 137.